

PHASE CURVE FITTING IN THE CONTEXT OF LARGE-SCALE PHOTOMETRIC SURVEYS

Colazo Milagros,

Dagmara Oszkiewicz, Alvaro Alvarez-Candal, Patrycja Poźniak,
Przemysław Bartczak, Edyta Podlewska-Gaca

Astronomical Observatory Institute, Faculty of Physics and Astronomy, AMU, Poland.
Instituto de Astrofísica de Andalucía, Spain.



What have we done?

Wilawer et al. (2024)

What are we doing?

Colazo et al. (2024, in prep)

What will we do?

PHASE CURVE WAVELENGTH DEPENDENCY AS REVEALED BY SHAPE- AND GEOMETRY-CORRECTED ASTEROID PHASE CURVES

DATA COLLECTION:

Dense differential ground-based data from the Astronomical Observatory Institute of Adam Mickiewicz University to model asteroids, focusing on their sidereal rotational period and spin axes.



Sparse ATLAS data were utilized to calculate photometric phase function parameters, assuming fixed asteroid shapes.

SELECTION CRITERIA:

35 asteroids with well-defined models, accurate periods, and pole coordinates based on photometric data from 11 previous studies.



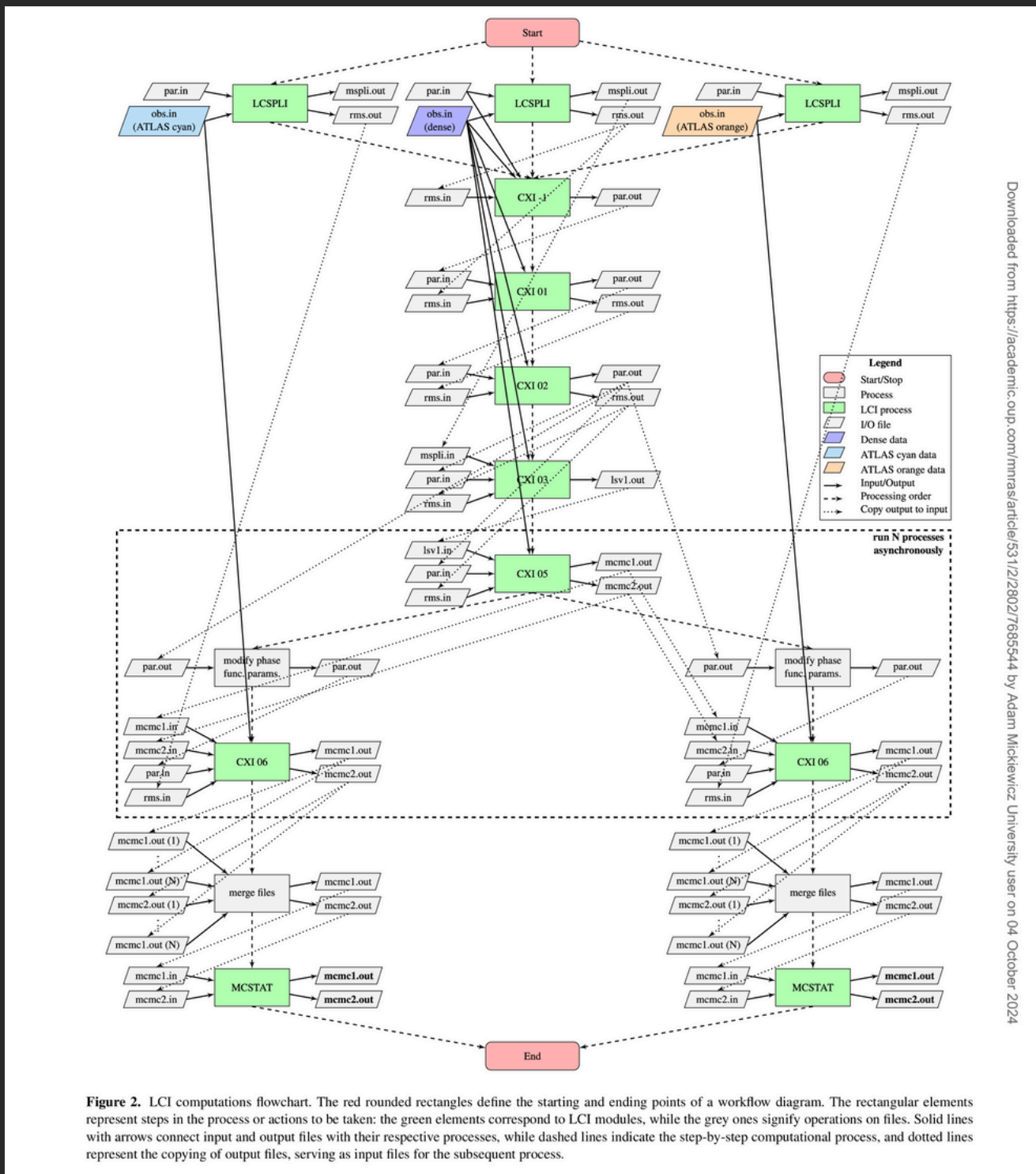
Muinonen et al (2022)



INVERSE PROBLEM FORMULATION

First Part: Solve the spin and shape parameters using dense, ground-based photometry without modeling the photometric phase function.

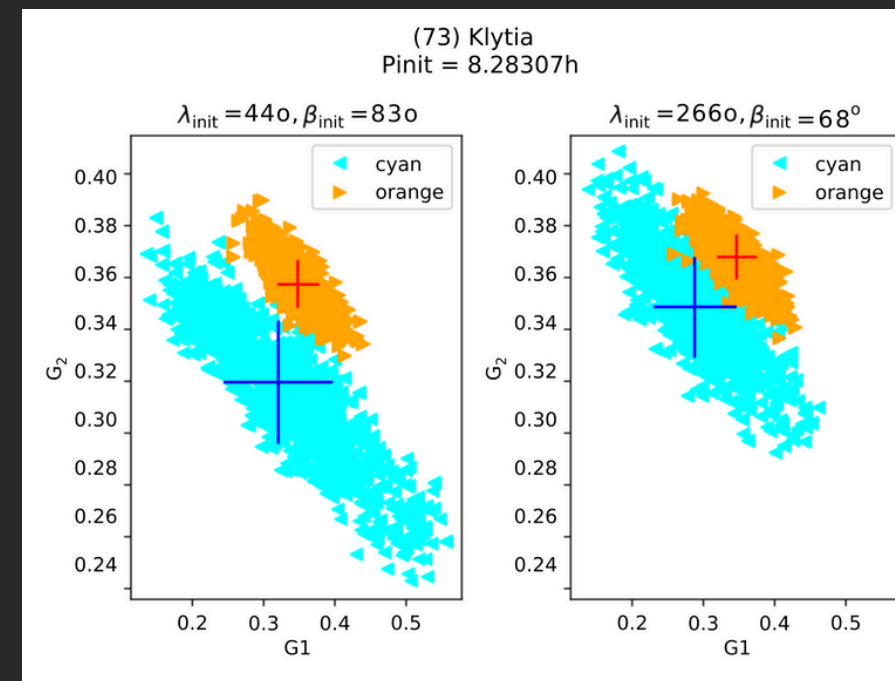
Second Part: Use the initial solutions to sample both photometric parameters (G1 and G2) along with the spin and shape parameters through MCMC.



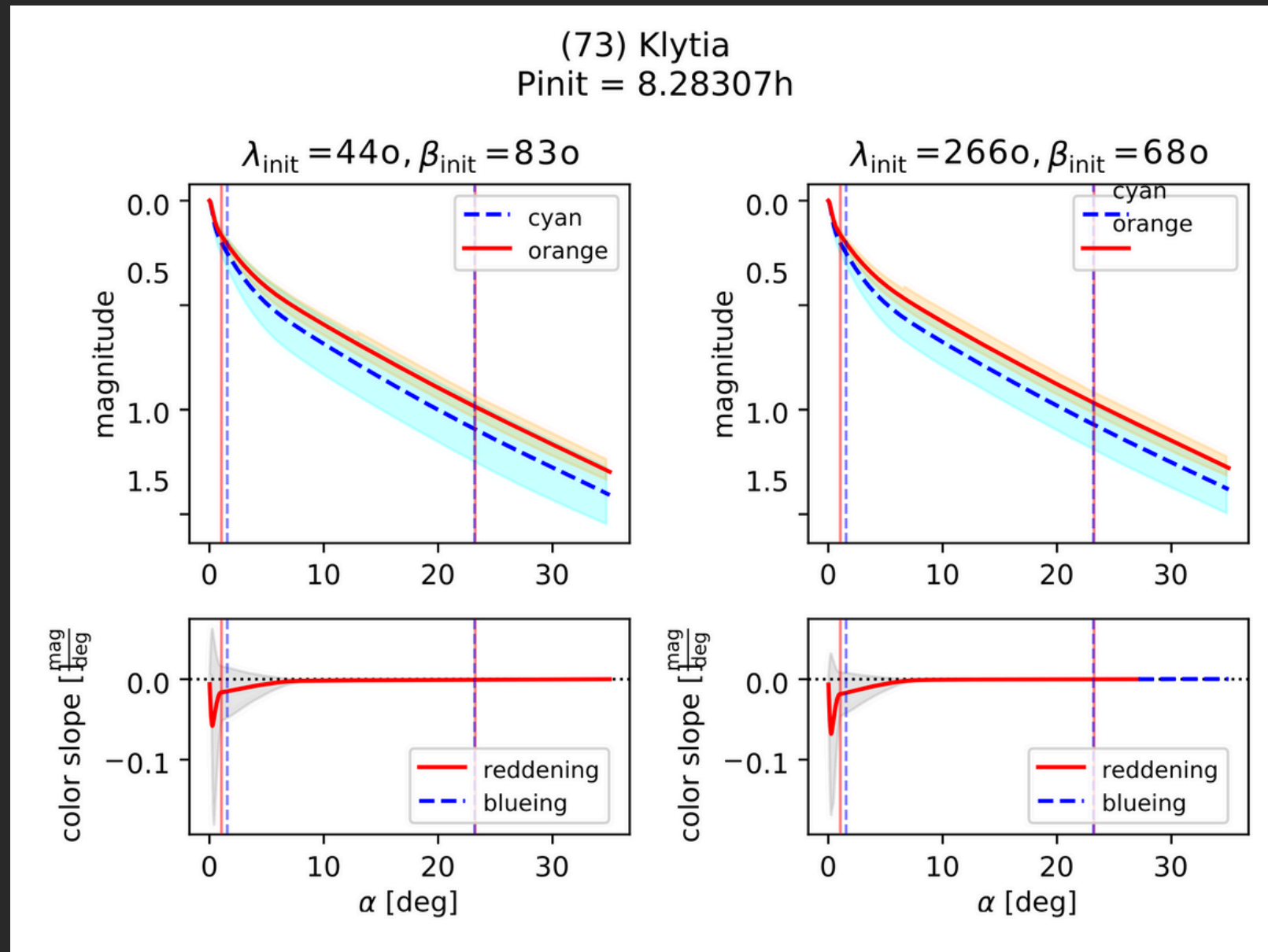
Downloaded from https://academic.oup.com/mnras/article/531/2/2802/7685544 by Adam Mickiewicz University user on 04 October 2024

Figure 2. LCI computations flowchart. The red rounded rectangles define the starting and ending points of a workflow diagram. The rectangular elements represent steps in the process or actions to be taken; the green elements correspond to LCI modules, while the grey ones signify operations on files. Solid lines with arrows connect input and output files with their respective processes, while dashed lines indicate the step-by-step computational process, and dotted lines represent the copying of output files, serving as input files for the subsequent process.

Adapted to a supercomputer at PCSS



PHASE CURVE WAVELENGTH DEPENDENCY AS REVEALED BY SHAPE- AND GEOMETRY-CORRECTED ASTEROID PHASE CURVES



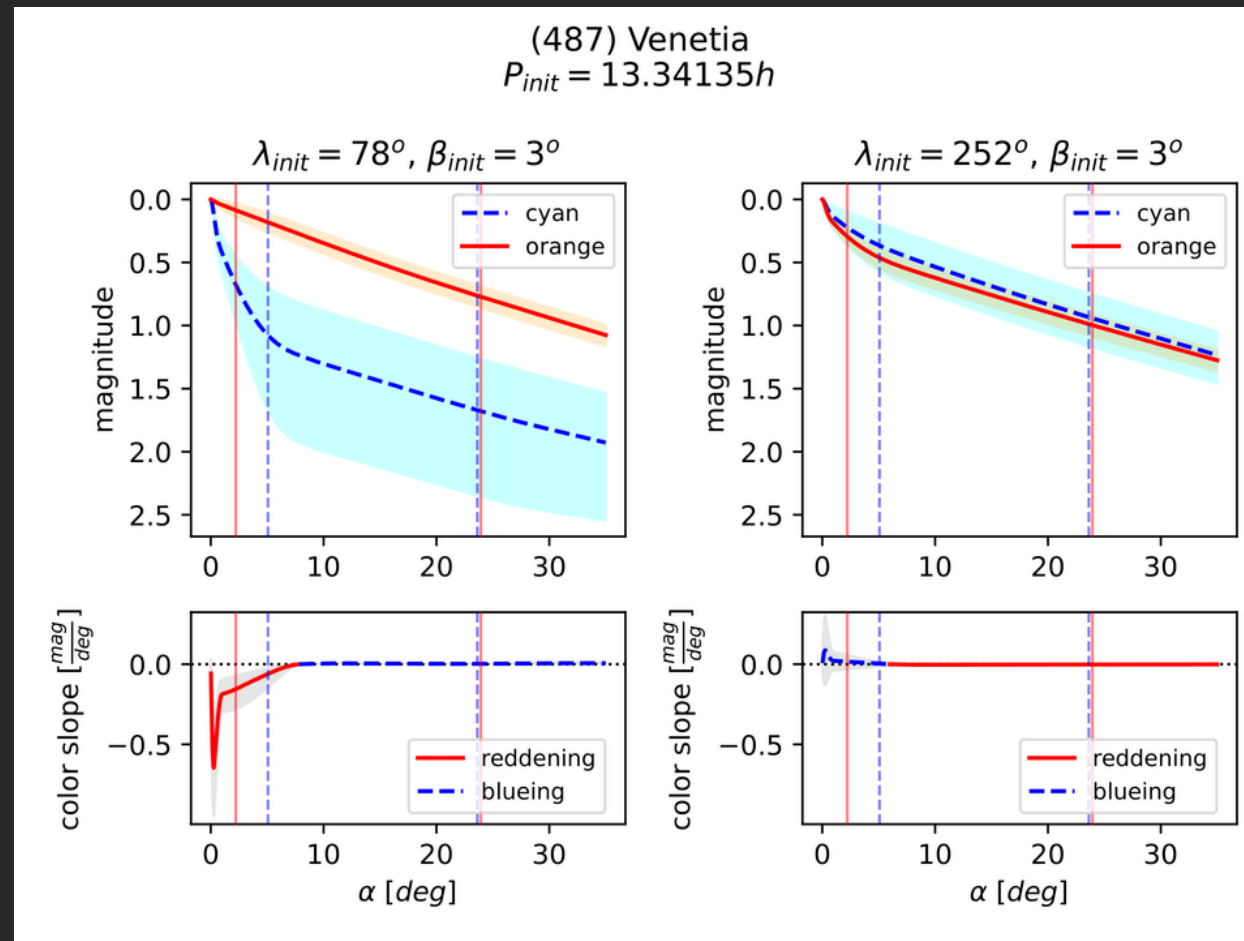
- Figures illustrate phase curves based on mean values of G1 and G2, with absolute magnitude H set to 0, and show the color slope as the difference in derivatives of the phase function in orange and cyan.
- Shaded areas represent 1-sigma uncertainties.
- A comparison of slopes indicates a reddening or blueing effect at small phase angles, but at angles above 10 degrees, the color slope is almost zero, making the effect negligible.



Highlights

- We analyze photometric properties of 35 asteroids using dense ground-based and sparse ATLAS survey data, focusing on two-color phase functions.
- The analysis of opposition effect amplitudes helps identify preferred rotational poles and reveals cases where phase curve parameters diverge from expected spectral types.

👿 Bad model ←



→ Good model 😊

Marciniak et al. (2018) identified the **second** solution as the preferred one, and our results are consistent with this, supporting the preferred solution.



Highlights

- We analyze photometric properties of 35 asteroids using dense ground-based and sparse ATLAS survey data, focusing on two-color phase functions.
- The analysis of opposition effect amplitudes helps identify preferred rotational poles and reveals cases where phase curve parameters diverge from expected spectral types.
- Distinct domains of G1 and G2 parameters emerge for cyan and orange filters, notably in some S-complex asteroids, where lower G2 values are observed in the cyan filter. The systematic effect in S-complex objects aligns with known albedo correlations: high albedo flattens phase curves, while low albedo steepens them.
 - Observed trend in a small sample — does it replicate in a statistically significant sample? 🙄
- For most asteroids, phase angle variations in orange-cyan color slope are strongest below 10 degrees, indicating more pronounced color effects at small angles.
- By correcting for shape and geometry, these refined phase curves enhance our understanding of asteroid surface properties, such as regolith and roughness. Yes, but: for 35 asteroids require **more than 170 000 hours of computations.**



ASTEROID PHASE CURVES AND REDDENING EFFECT USING ATLAS SURVEY DATA

We use the H, G1, G2 phase function developed by Muinonen et al. (2010), but in a multi-opposition fitting approach.

The magnitude data are converted to flux and divided into different filters. The fitting process is nonlinear and performed in the flux domain. The flux is obtained from:

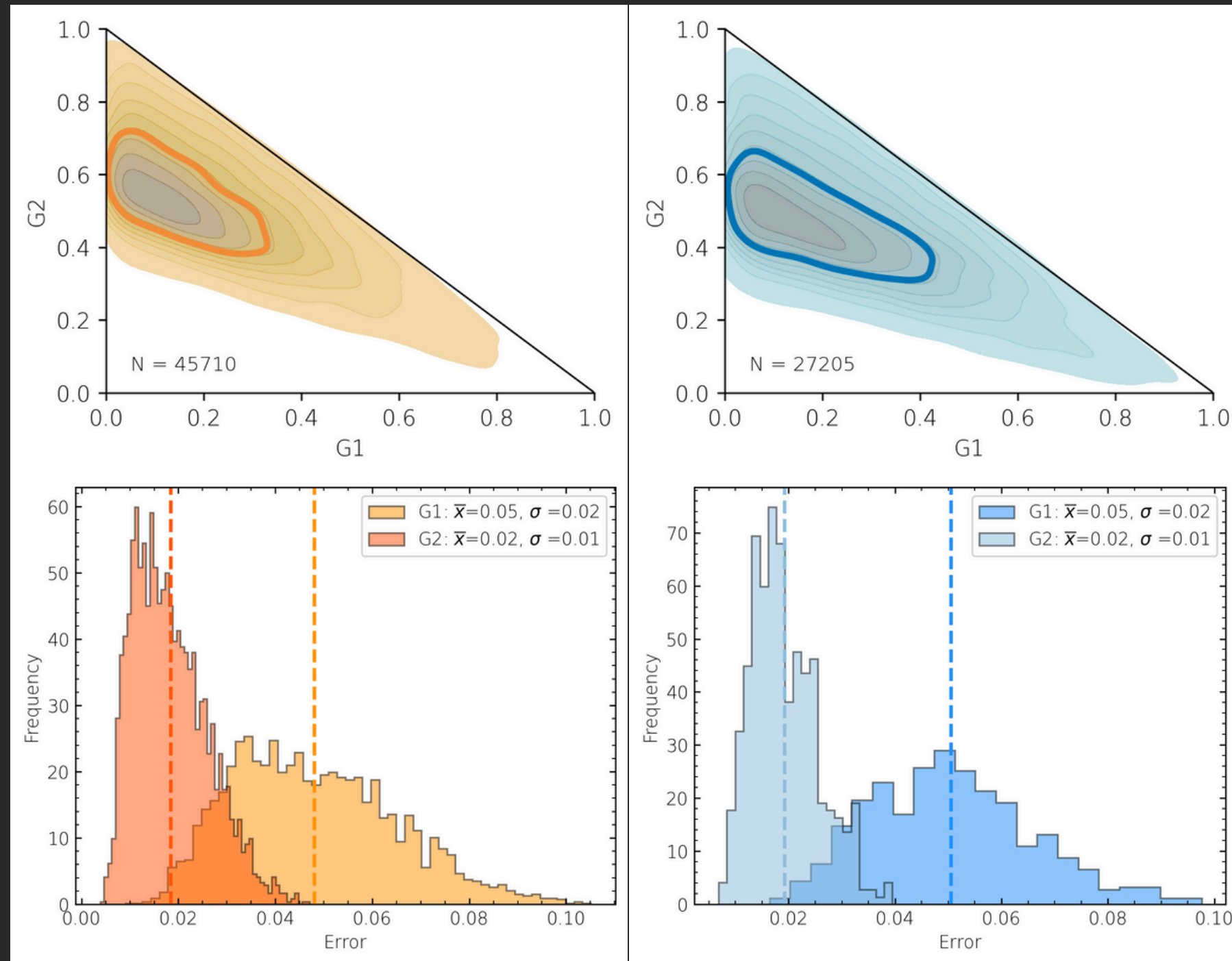
$$10^{-0.4V(\alpha)} = \sum_{i=1}^N 10^{-0.4H_i} [G_1\phi_1(\alpha) + G_2\phi_2(\alpha) + (1 - G_1 - G_2)\phi_3(\alpha)]$$

The data are **split into different oppositions** using solar elongation information downloaded from the JPL Horizons system using the Python astroquery package.

For each filter, the data from various oppositions are fitted simultaneously, using the same G1 and G2 parameters but different absolute magnitudes H for each apparition.

ASTEROID PHASE CURVES AND REDDENING EFFECT USING ATLAS SURVEY DATA

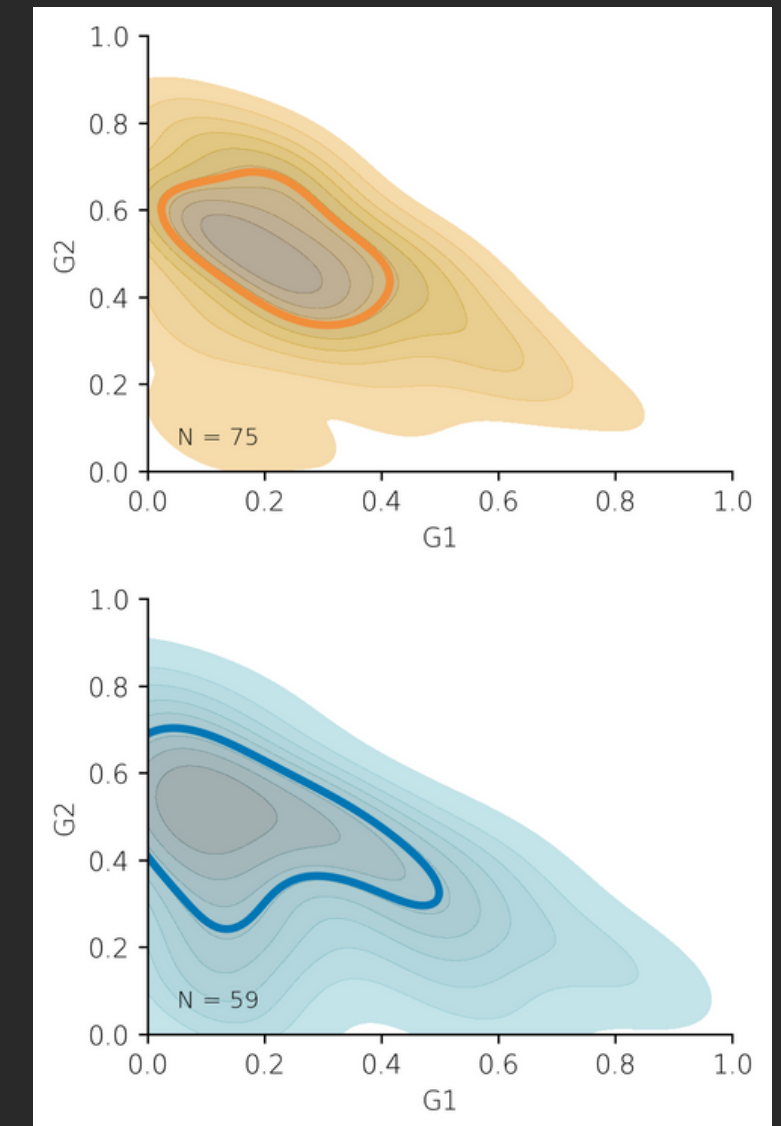
DATA: ATLAS Solar System Catalog V2 (2024-05-29)



The G2 parameter consistently presents lower uncertainties than the G1 parameter.



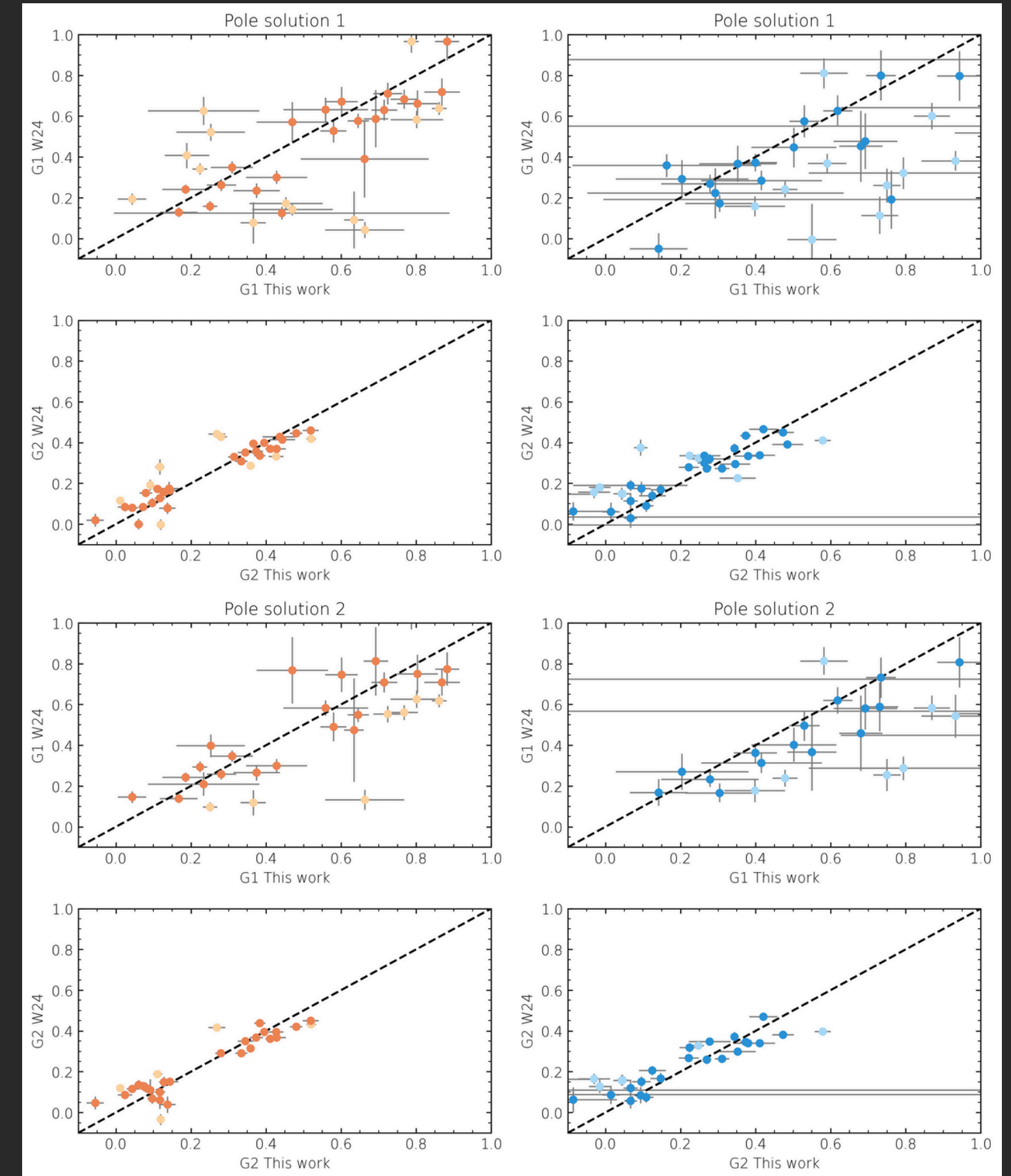
NEAs



COMPARISON WITH OTHER METHODS

Wilawer et al. (2024)

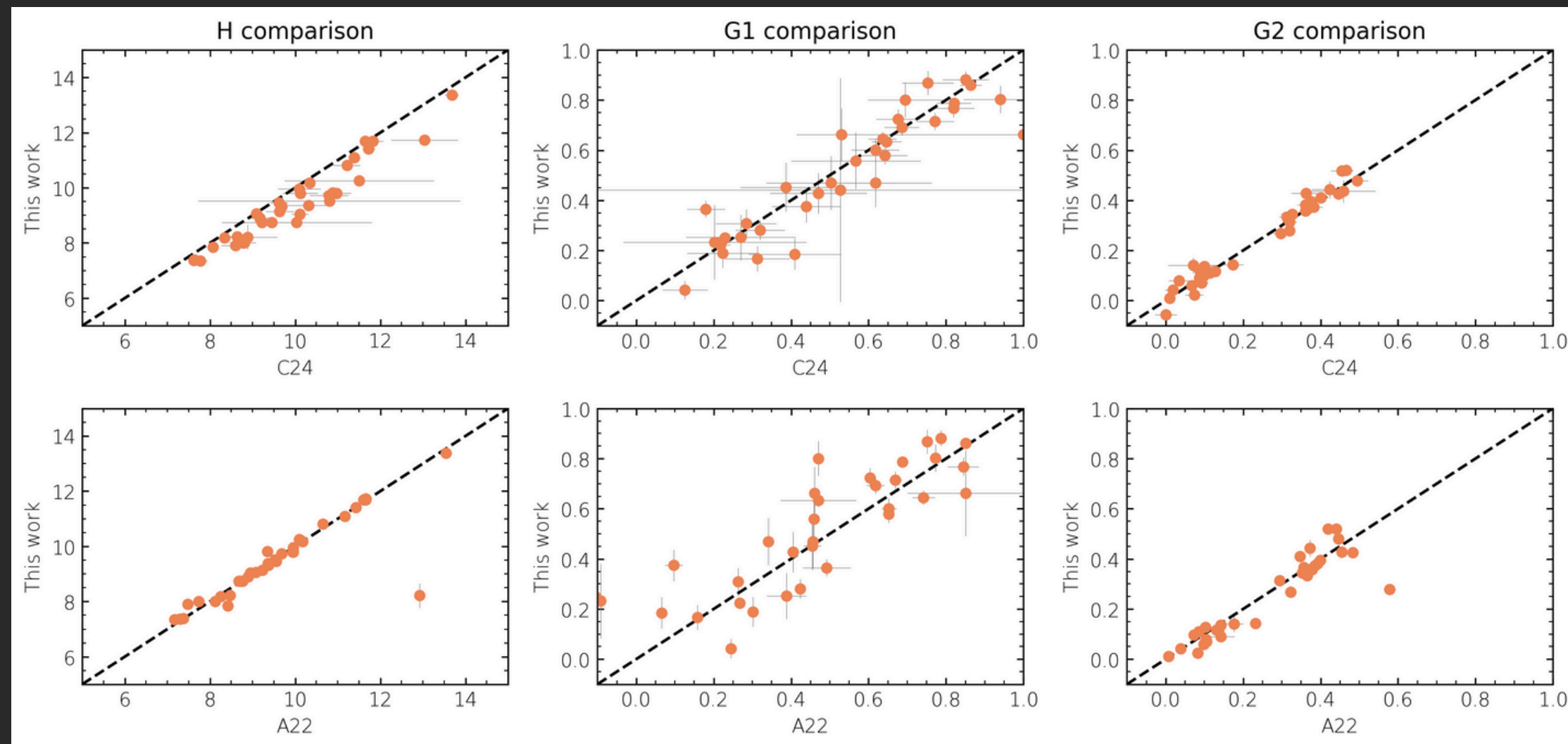
- W24 used ATLAS and ground-based data to derive phase curves for 35 well-observed asteroids, incorporating complex processes like fixed-shape modeling and dense rotational data. Their method required about **170 000 hours** of computational time, including supercomputer adaptations.
- Our approach is simpler and excludes some effects like rotational correction.
- It is designed for scalability when working with around 700,000 objects. Our algorithm takes **1 minute** to perform the outlier rejection and phase curve fitting for a sample of 35 asteroids using ATLAS observations.
- Our results are similar to W24, with most values within uncertainty intervals.
- Significant deviations occur in known challenging cases. Differences in G1 values are particularly noticeable for objects with sparse data near opposition.



Comparison with other methods

Carry et al. (2024)

- Proposed a phase function model that considers variability between apparitions and adds a term for asteroid orientation, oblateness, and equatorial coordinates.
- Their results are similar to ours, suggesting that their approach of separating by apparitions or adding the orientation term is comparable to our method.
- Their absolute magnitudes (H) are slightly brighter, likely due to biases in the data to which our method is sensitive, resulting in differences in H values compared to other methods that account for spin and shape corrections.

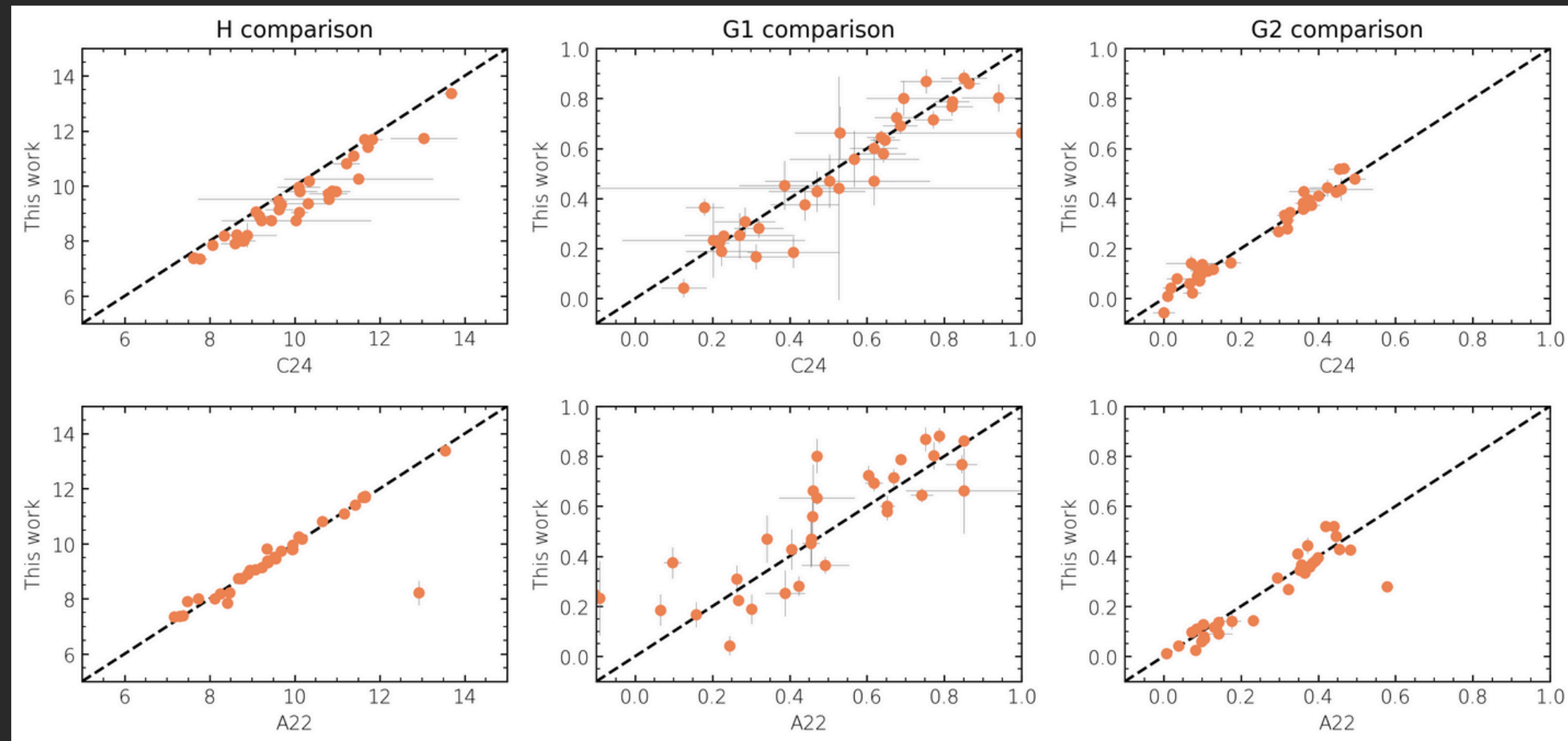


↓
For NEAs, the average change in H for different oppositions is 0.22 mag.

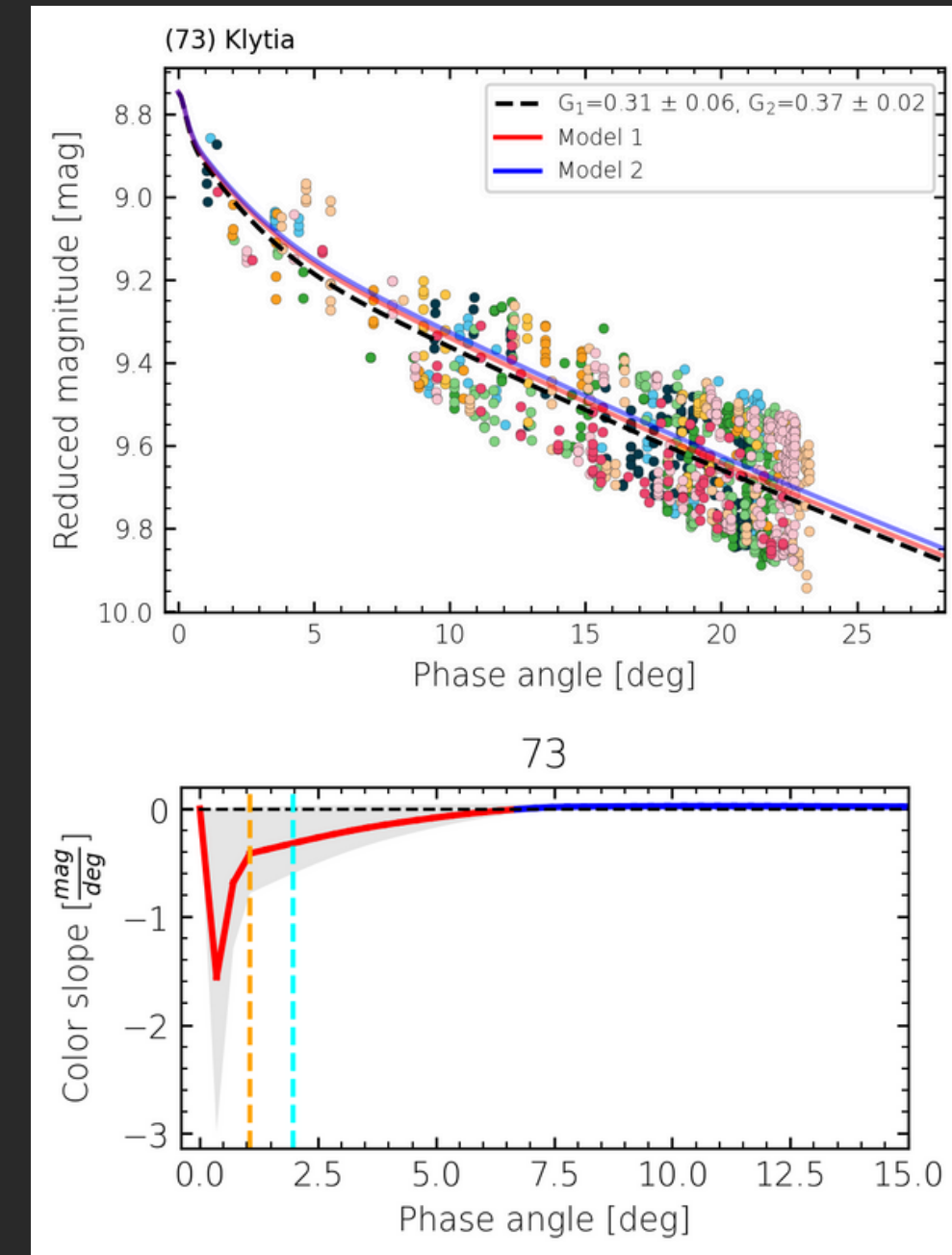
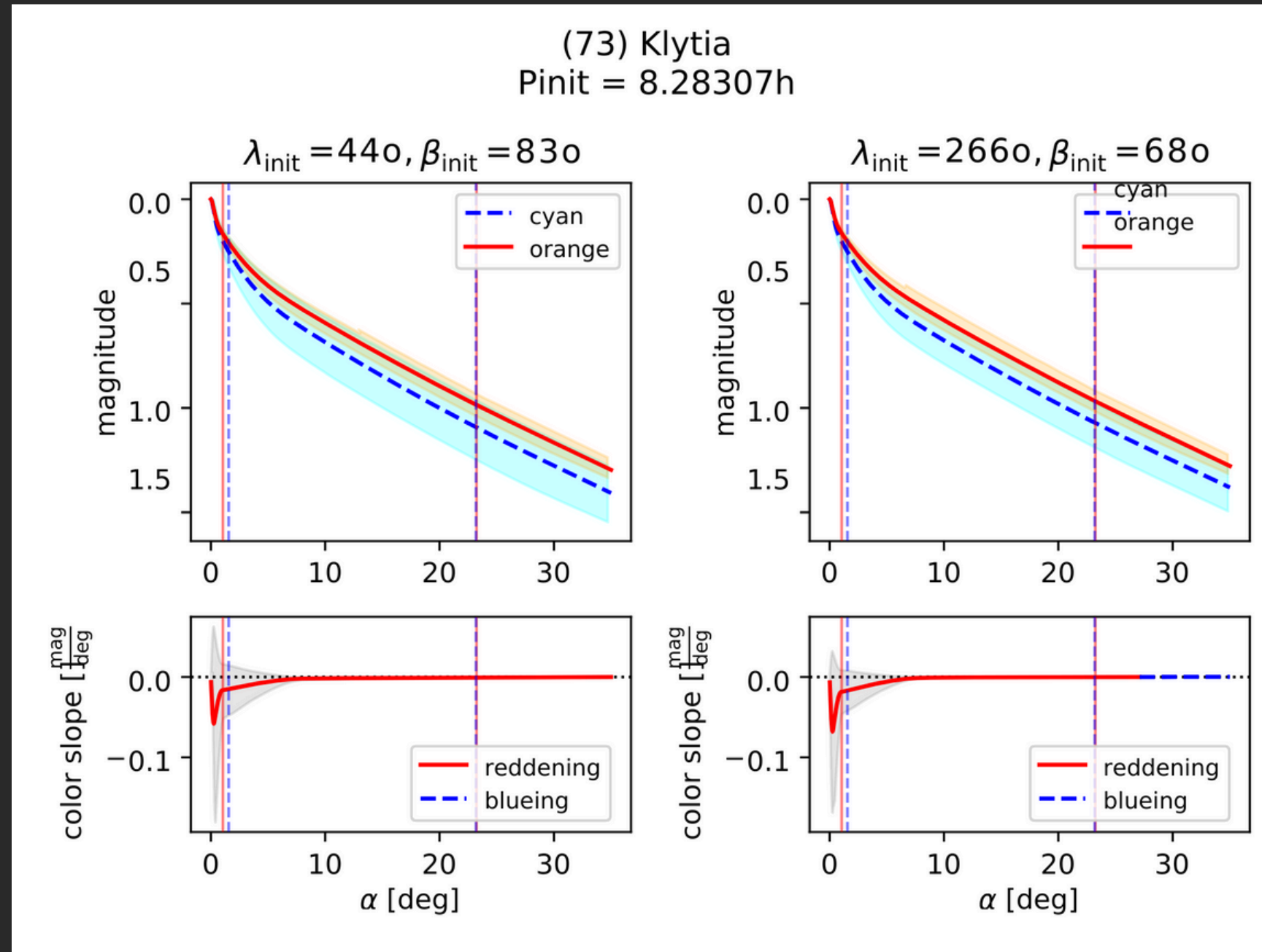
Comparison with other methods

Álvarez-Candal et al. (2022)

- Used Monte Carlo simulations and Bayesian inference, incorporating errors in magnitudes and rotational variations.
- Their results are consistent with ours, including H values.
- Their method took 32 minutes for 1000 MC iterations, while ours took about 1 minute for 35 asteroids per filter.

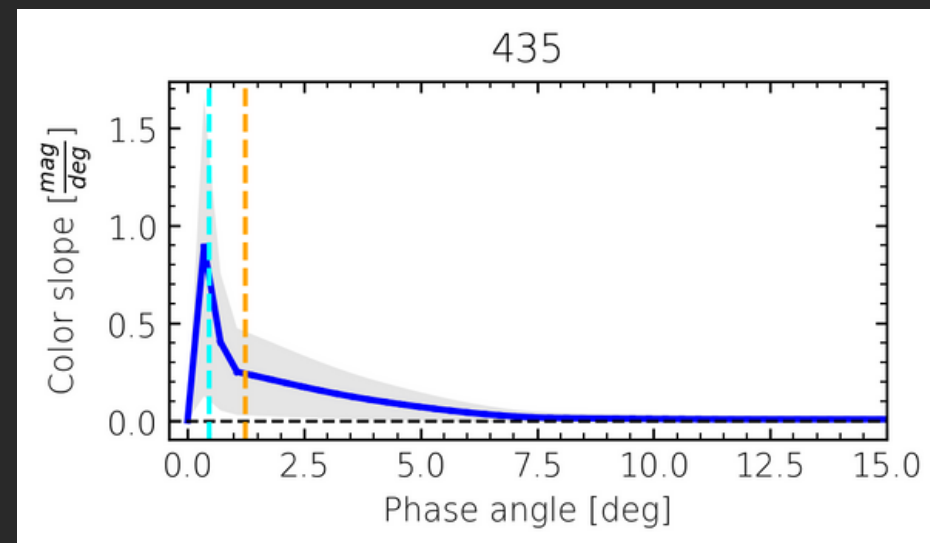
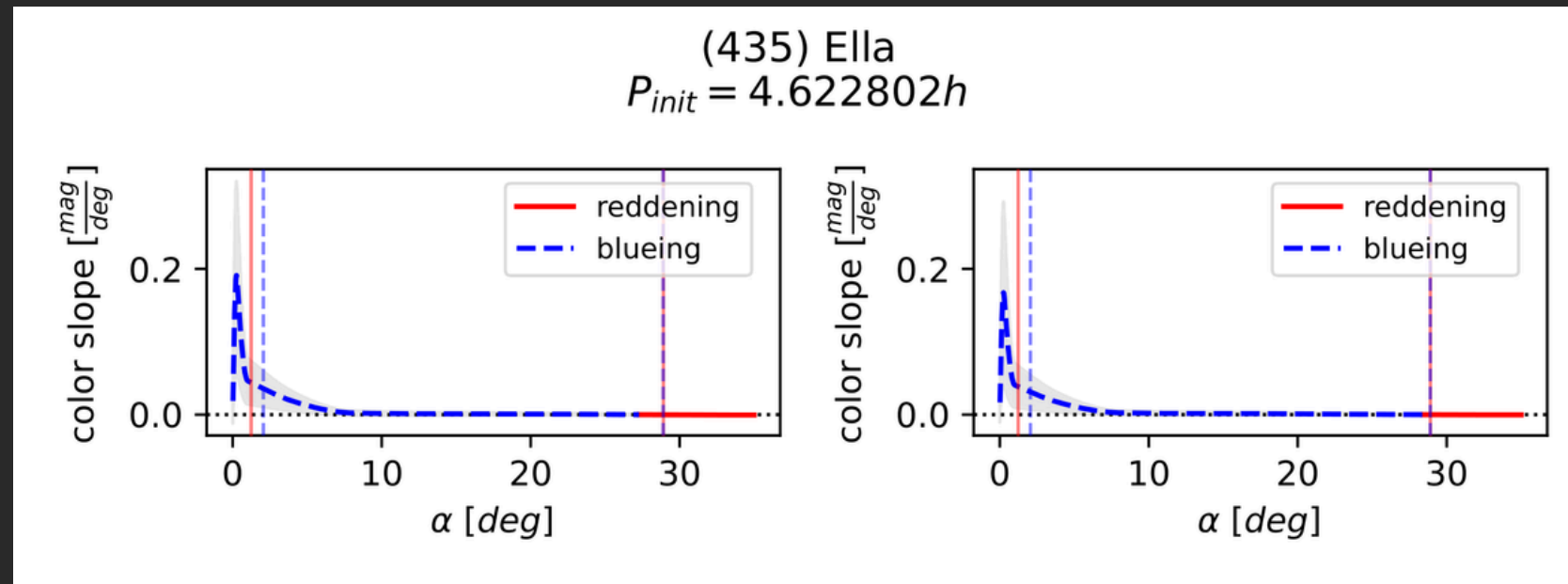


Phase coloring

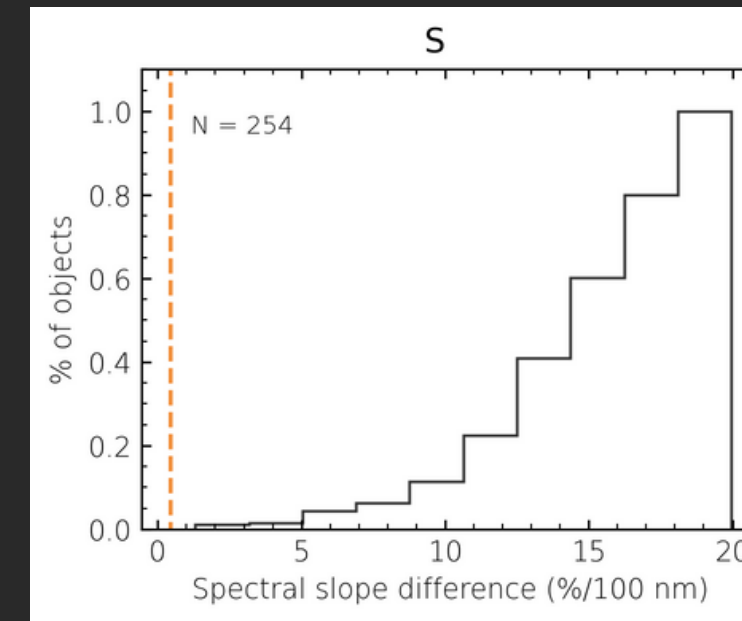


Phase coloring

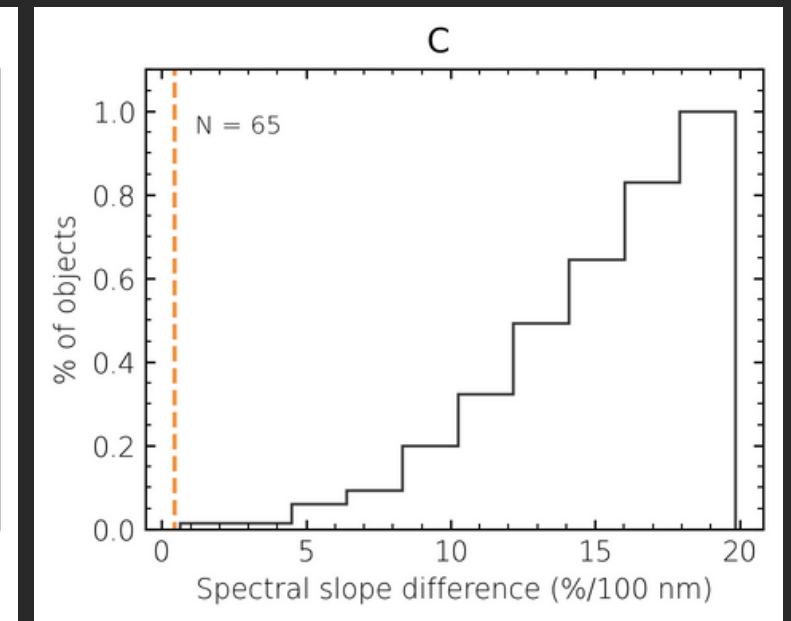
For phase angles below ~5 degrees:



6.45%



5.38%

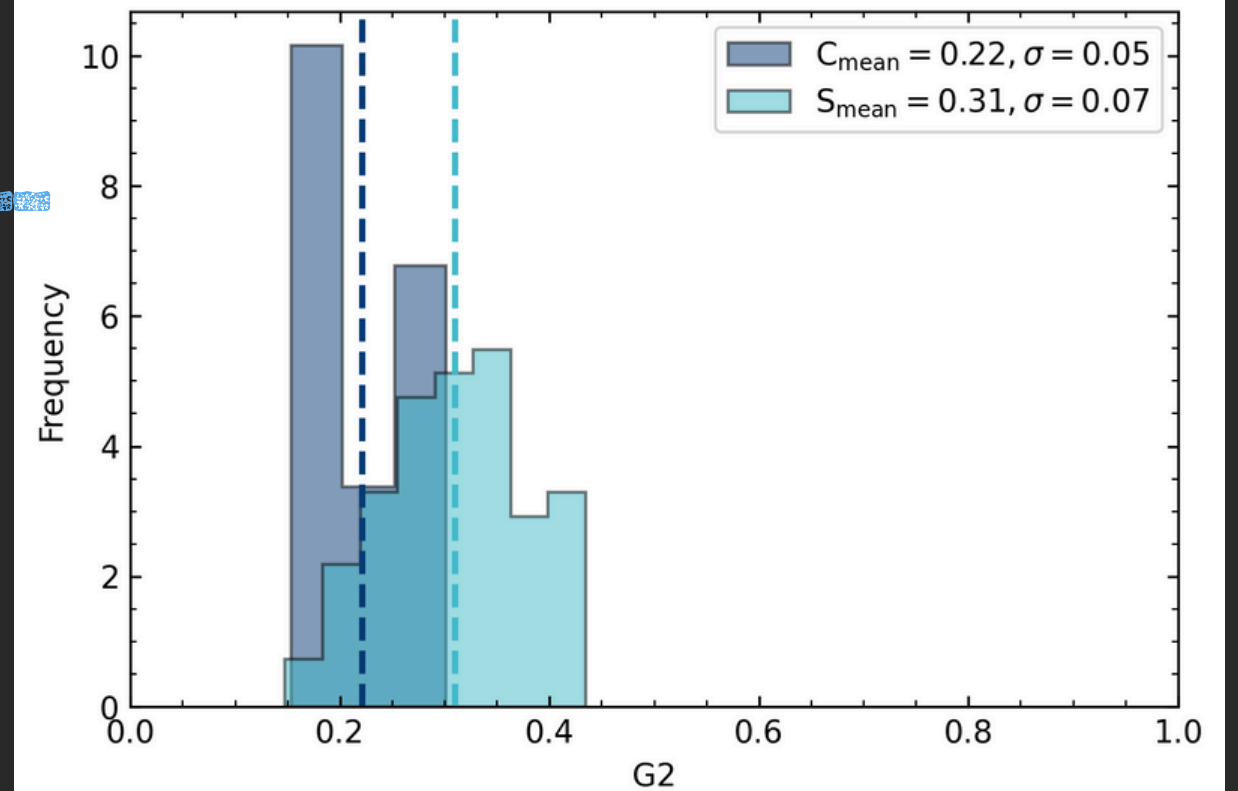
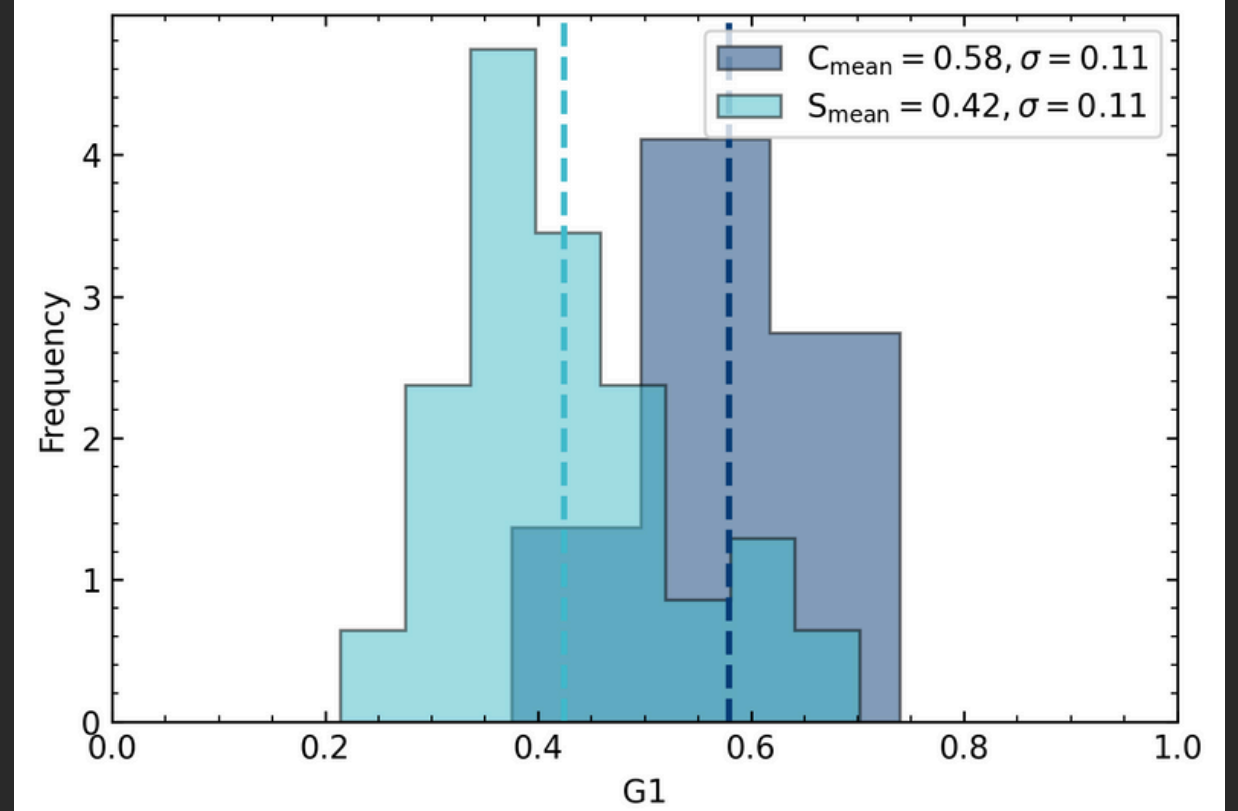
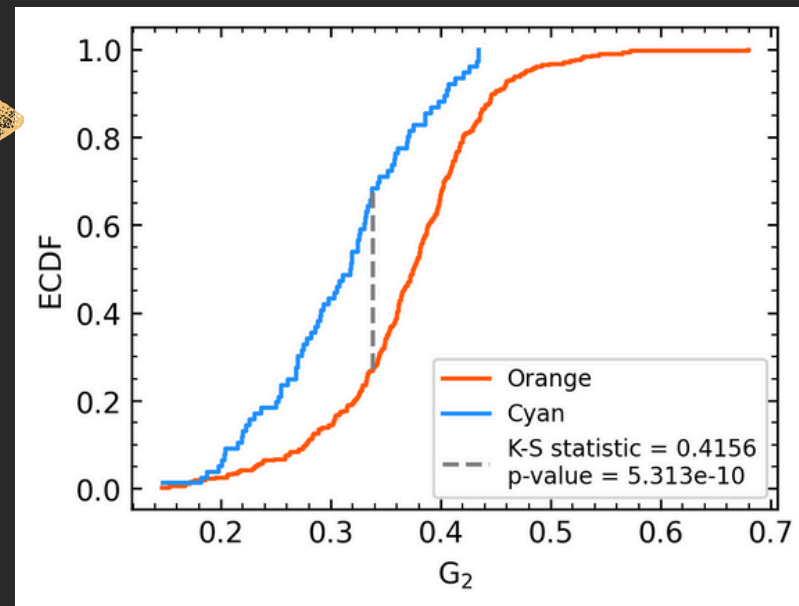
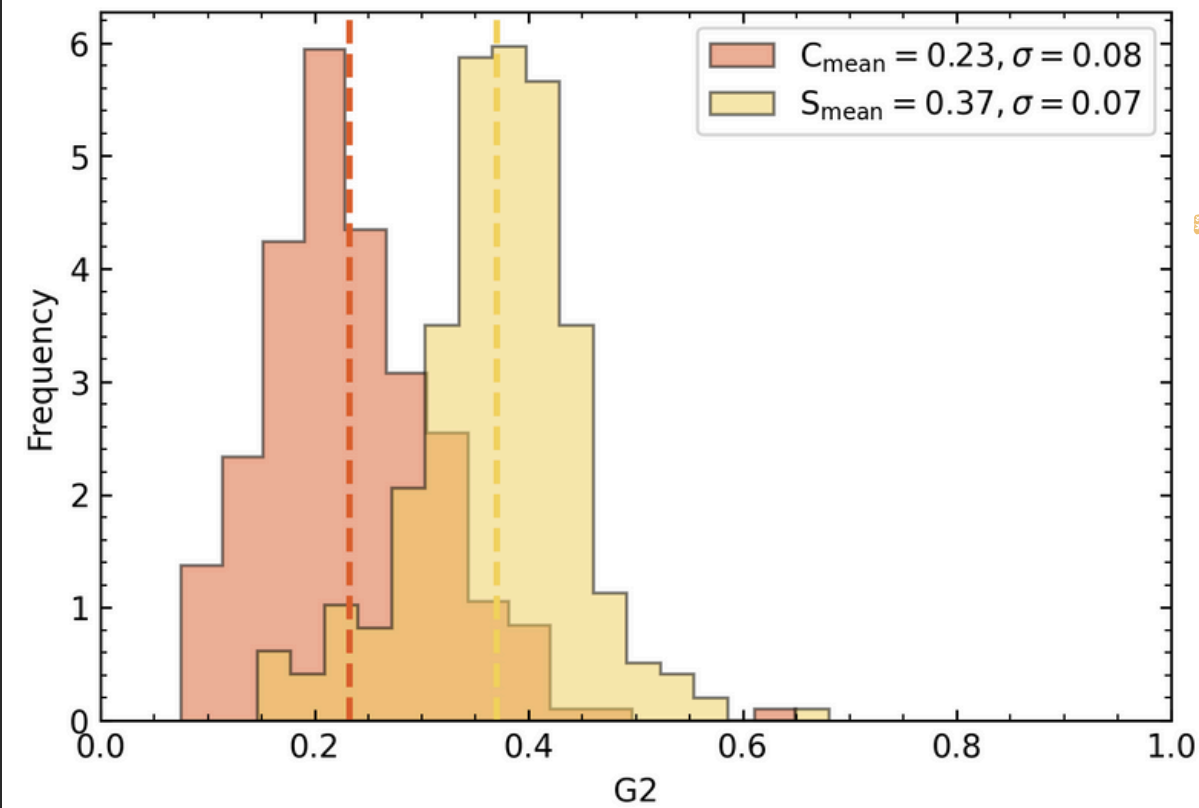
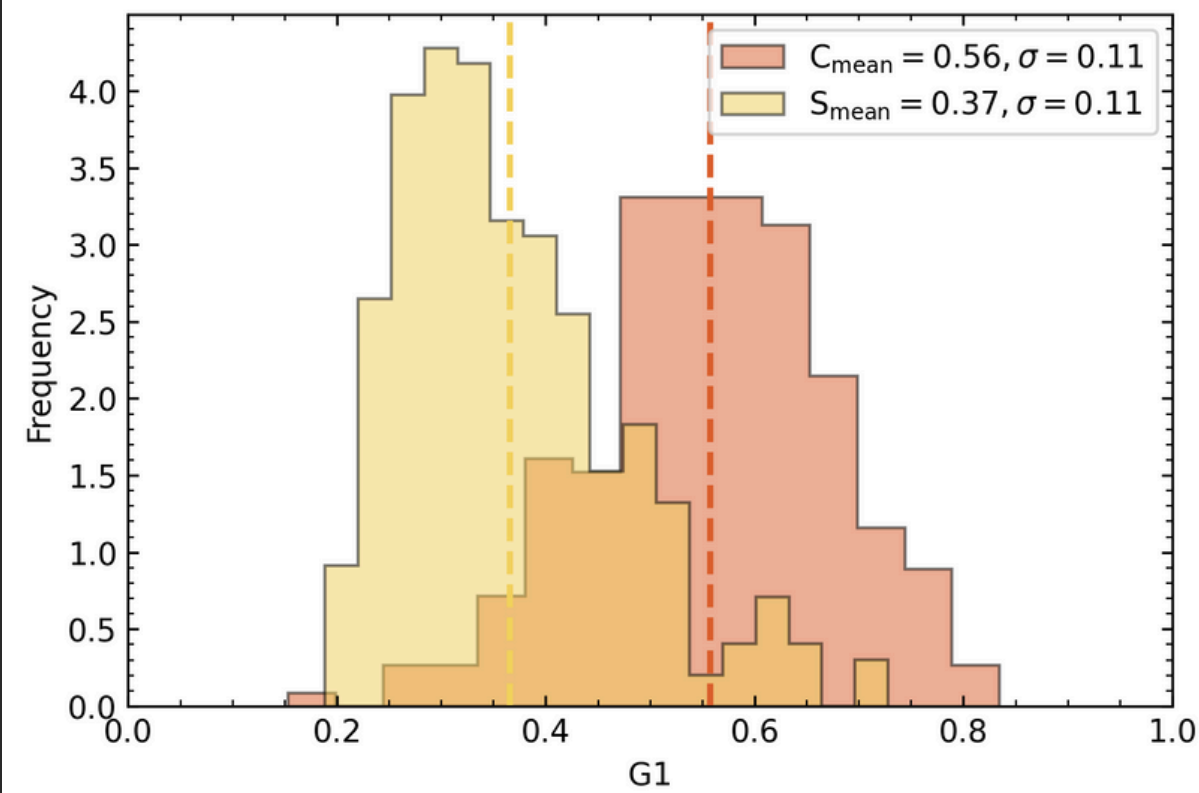


Small percentages of asteroids show phase reddening when comparing the spectral slopes over the cyan to orange within the phase angle range of 10–30 degrees.

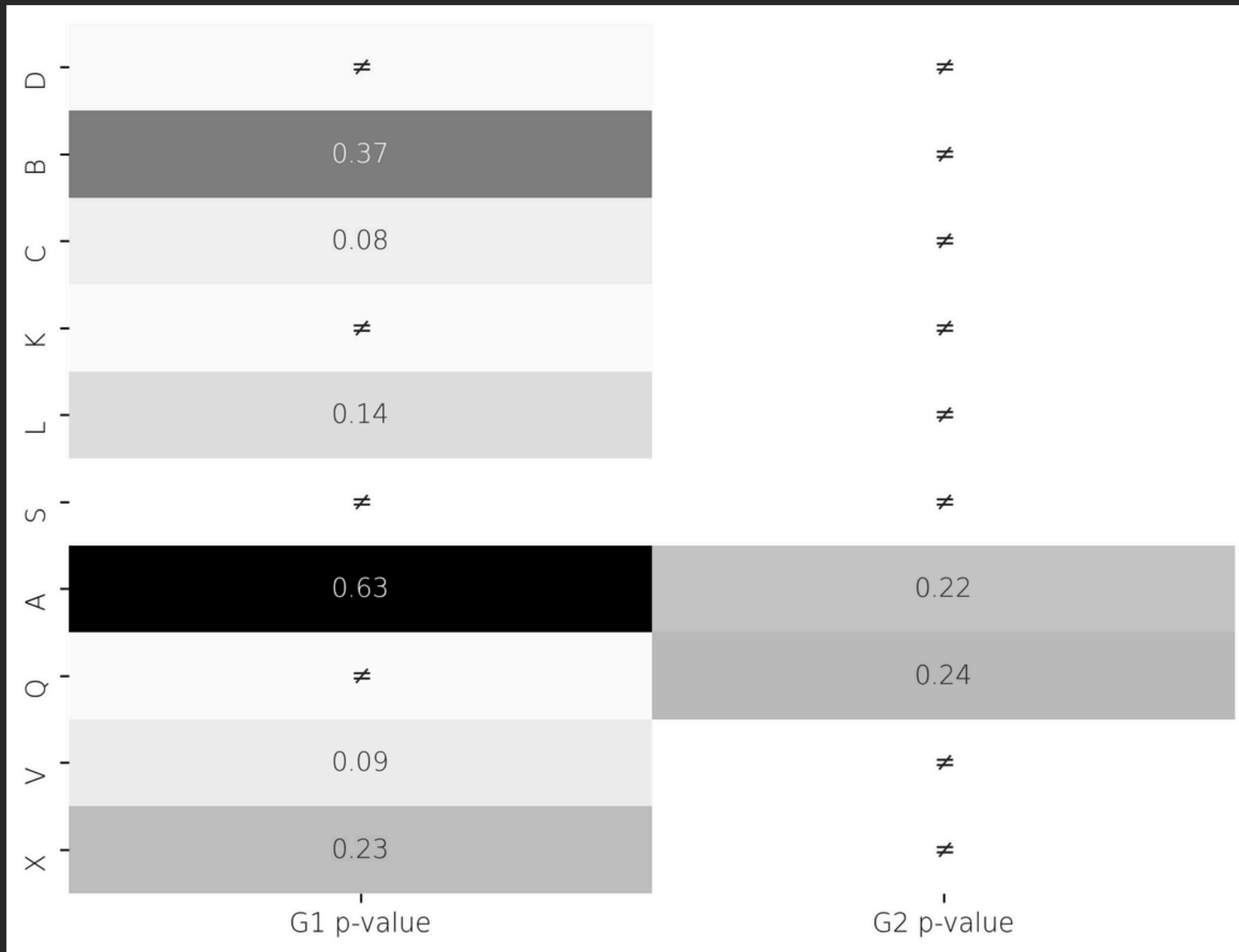
ASTEROID PHASE CURVES AND REDDENING EFFECT USING ATLAS SURVEY DATA

TAXONOMY

The mean G2 values for C-type asteroids are similar in both filters. However, the mean G2 value for the S-complex is lower in the cyan filter, as also noted by Wilawer et al. (2024)



TAXONOMY



K-S Tests between G1(o) - G1(c) and G2(o) - G2(c) for the same taxonomic type.

- Statistically significant differences in G1 and G2 values are observed across filters for the D, K, and S complexes, indicating wavelength dependency.
- The A complex shows no significant differences across filters.
- Notably, variations in the G2 parameter are greater than those in G1 across complexes.

Highlights

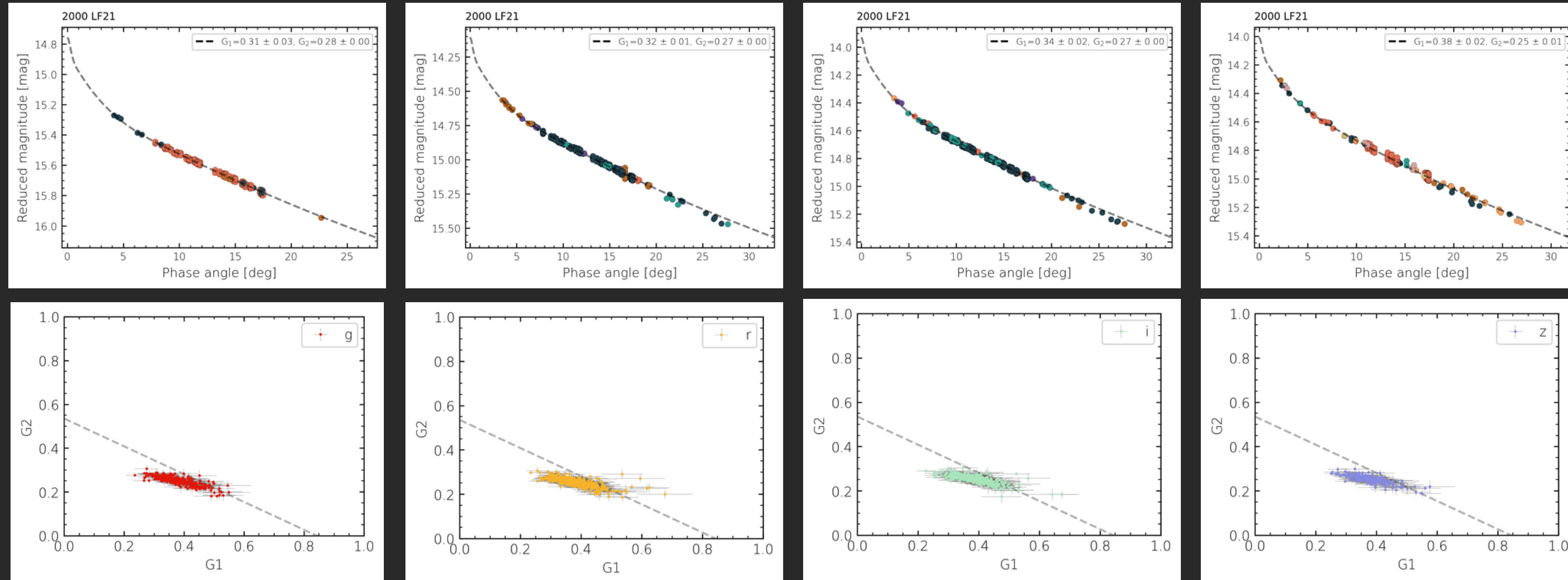
- **Phase Curve Analysis:** We determined phase curves for $> 270\,000$ asteroids.
- **Taxonomy Cross-Matching:** By combining our data with taxonomy databases, we observed that S- and V-type asteroids generally fall in the $G1 < G2$ region, indicative of higher albedo. In contrast, darker C- and B-types cluster in the $G1 > G2$ region. Filter dependence was minimal for C-types but evident in S-types, where phase curves in the cyan filter were flatter (KS-test).
- **Phase Coloring Analysis:** Small percentages of asteroids show phase reddening when comparing the spectral slopes over the cyan to orange within the phase angle range of 10–30 degrees. This aligns with the expectation that reddening effects become more noticeable at higher phase angles. However, ATLAS filters' narrow wavelength range and the absence of rotational corrections in our method may limit color detection. Nonetheless, phase coloring appears noticeable at phase angles below 5 degrees.

Highlights

- **Uncertainty Patterns:** The G2 parameter consistently shows lower uncertainty than G1. Simulations confirm that G2 is less affected by phase angle coverage. G1, however, is sensitive to the opposition region and changes significantly with additional data.
- **Computational Efficiency:** Our approach is highly efficient, processing parameters for 35 asteroids in one minute, whereas a more complex method may require up to 170 000 hours. This efficiency is critical in large surveys where a balance between accuracy and speed is essential.
- **Method Comparison:** We compared our method with those of Wilawer et al. (2024), Carry et al. (2024) and Alvarez et al. (2022). Results were generally similar.
- **Algorithm Adaptability:** Our approach is adaptable to various datasets, including LSST data. Preparations are underway to adapt it using simulated data from Data Preview 0.3, showing potential for future large-scale datasets.

ASTEROID PHASE CURVES AND REDDENING EFFECT USING ATLAS SURVEY DATA

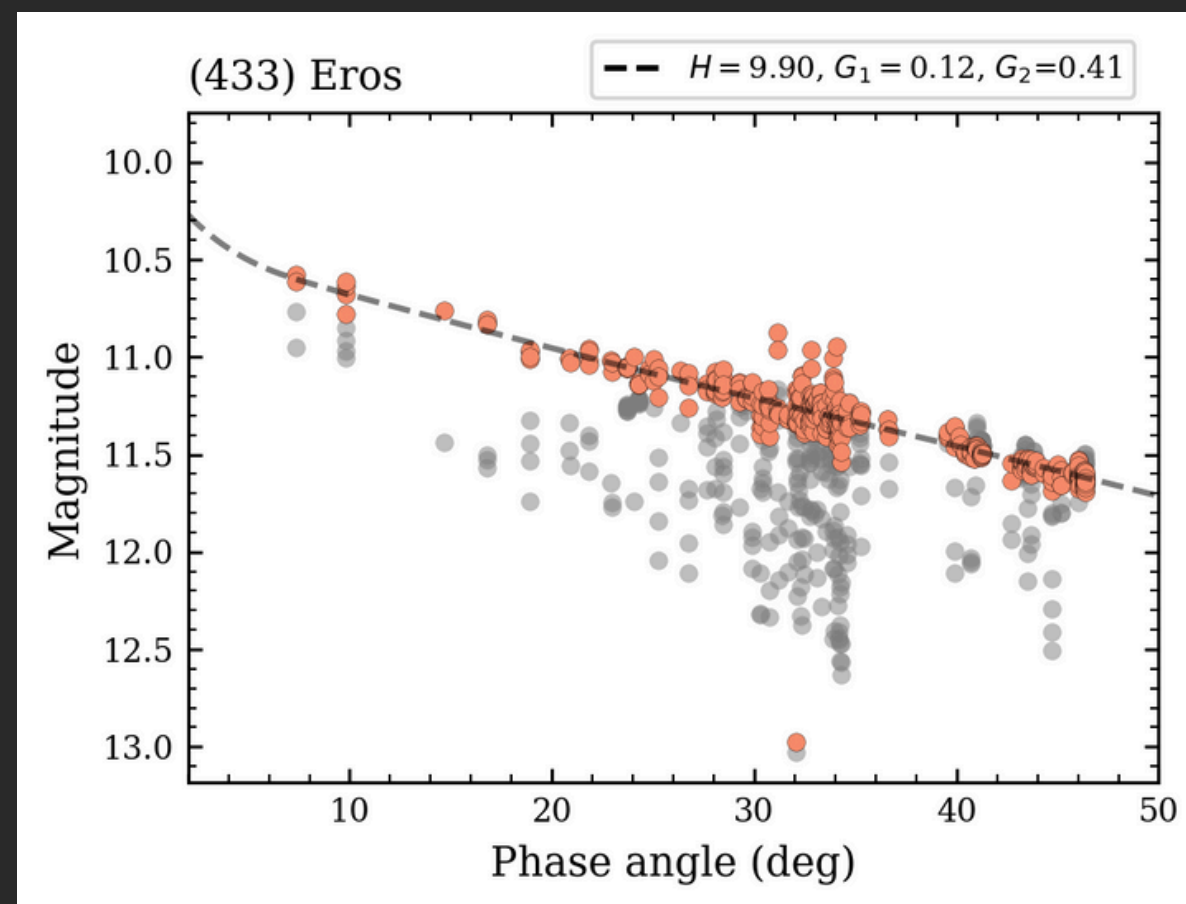
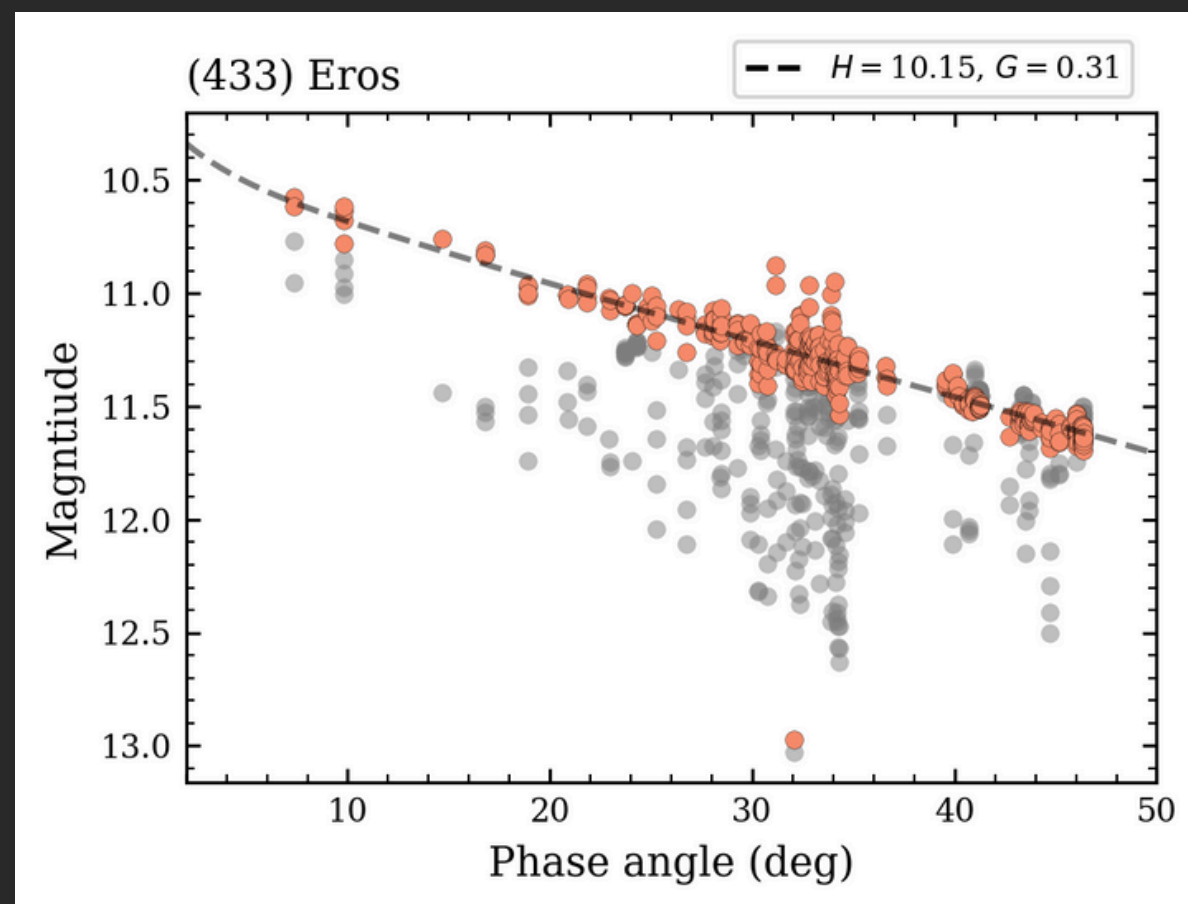
Highlights



- **Algorithm Adaptability:** Our approach is adaptable to various datasets, including LSST data. Preparations are underway to adapt it using simulated data from Data Preview 0.3, showing potential for future large-scale datasets.

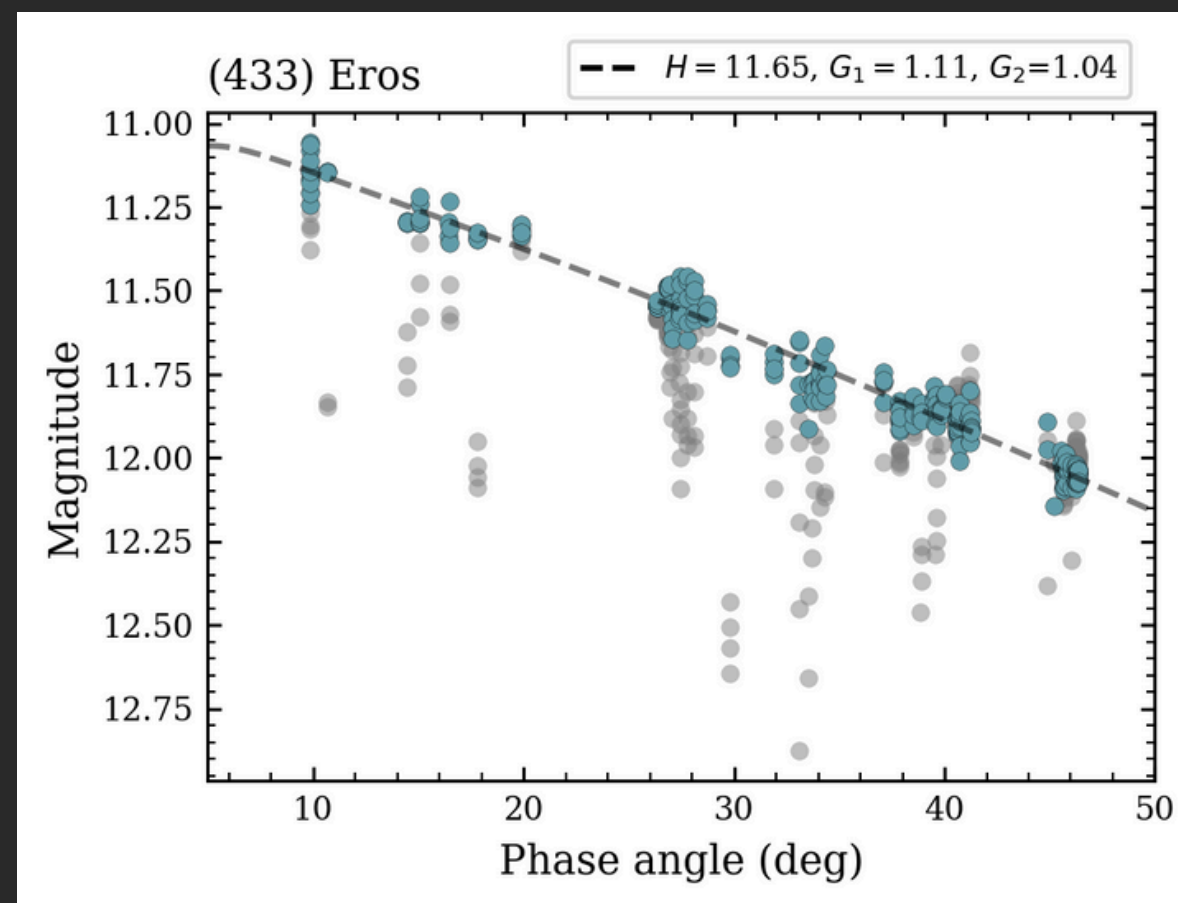
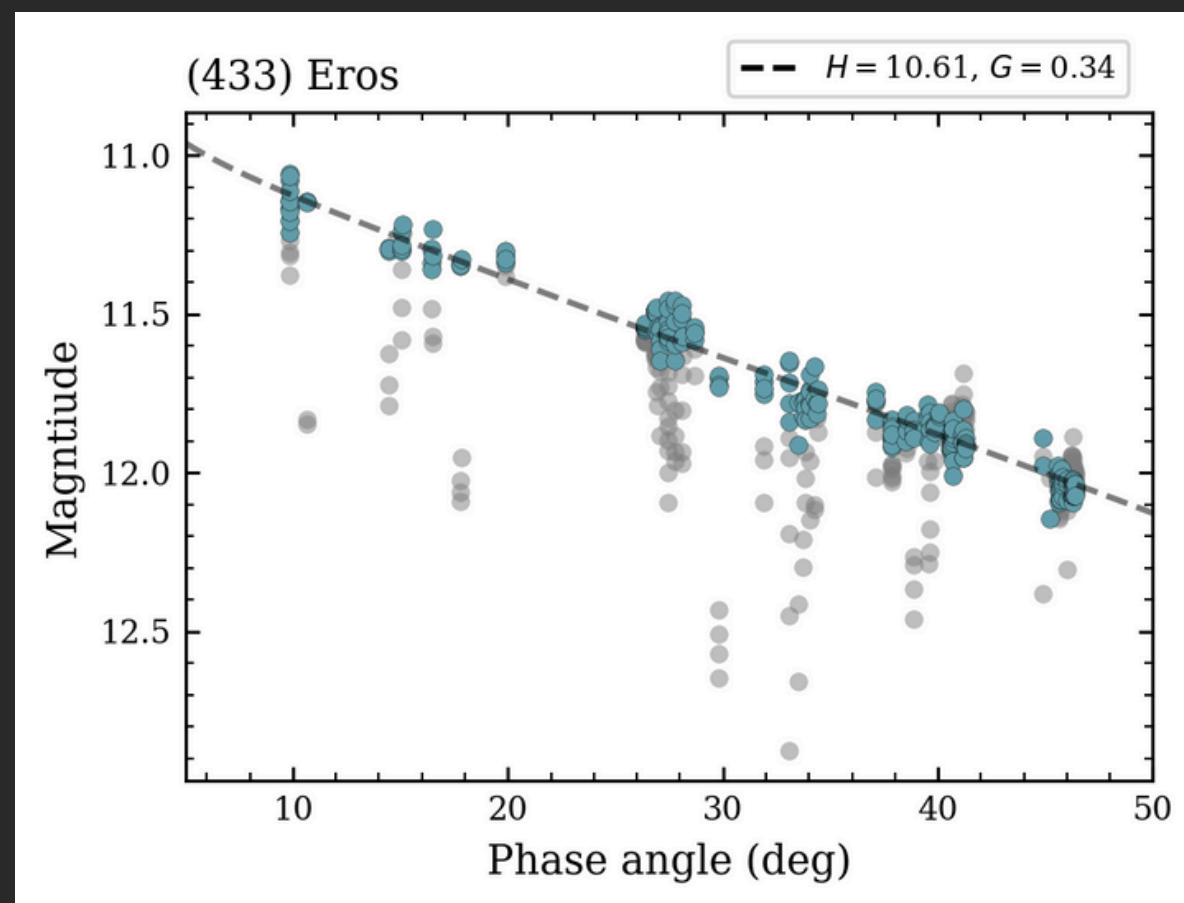
CELLINOID MODEL

- Our model primarily relies on the cellinoid model but can also incorporate shape models derived from space missions and other sources.
- This empirical model estimates the brightness difference between the observed and reference geometries, which is then removed from the data.
- This approach differs slightly from Carry et al. (2024) methodology, focusing on geometry-based brightness corrections.



CELLINOID MODEL

- Our model primarily relies on the cellinoid model but can also incorporate shape models derived from space missions and other sources.
- This empirical model estimates the brightness difference between the observed and reference geometries, which is then removed from the data.
- This approach differs slightly from Carry et al. (2024) methodology, focusing on geometry-based brightness corrections.



FINAL THOUGHTS

Today, we have an astonishing amount of asteroid data, and with more surveys on the horizon, the data flood we'll receive will be immense.

- ARE WE PREPARED FOR THIS?
- ARE OUR ALGORITHMS SCALABLE ENOUGH TO HANDLE IT?
- WHAT TRADE-OFF BETWEEN COMPUTATIONAL COST AND PRECISION ARE WE WILLING TO ACCEPT?
- HOW MUCH CAN WE EXPECT FROM OUR SPARSE DATA? WHAT KIND OF SCIENCE WILL WE BE ABLE TO ACHIEVE IN THIS ERA OF MASSIVE DATA?

These are the questions we should answer if we want to make the most of this new era in astronomical observation.



Thank you!